



OPEN ACCESS

EDITED BY
Xuezhong Yang,
University of Chinese Academy of
Sciences, China

REVIEWED BY
Muye Li,
University of Chinese Academy of
Science, China
Baitao Zhang,
Shandong University, China

*CORRESPONDENCE
Huadong Lu,
luhuadong@sxu.edu.cn

SPECIALTY SECTION
This article was submitted to Optics and
Photonics,
a section of the journal
Frontiers in Physics

RECEIVED 27 August 2022
ACCEPTED 20 September 2022
PUBLISHED 06 October 2022

CITATION
Jin P, Wei J, Su J, Lu H and Peng K
(2022), Recent progress in continuously
tunable low-noise all-solid-state single-
frequency continuous-wave laser based
on intracavity locked etalon.
Front. Phys. 10:1029336.
doi: 10.3389/fphy.2022.1029336

COPYRIGHT
© 2022 Jin, Wei, Su, Lu and Peng. This
is an open-access article distributed
under the terms of the [Creative
Commons Attribution License \(CC BY\)](#).
The use, distribution or reproduction in
other forums is permitted, provided the
original author(s) and the copyright
owner(s) are credited and that the
original publication in this journal is
cited, in accordance with accepted
academic practice. No use, distribution
or reproduction is permitted which does
not comply with these terms.

Recent progress in continuously tunable low-noise all-solid-state single-frequency continuous-wave laser based on intracavity locked etalon

Pixian Jin^{1,2}, Jiao Wei^{1,2}, Jing Su^{1,2}, Huadong Lu^{1,2*} and Kunchi Peng^{1,2}

¹State Key Laboratory of Quantum Optics and Quantum Optics Devices, Institute of Opto-Electronics, Shanxi University, Taiyuan, China, ²Collaborative Innovation Center of Extreme Optics, Shanxi University, Taiyuan, Shanxi, China

All-solid-state single-frequency continuous-wave (CW) lasers have been applied in many fields of scientific research owing to their intrinsic advantages of high beam quality, low noise, narrow linewidth, and high coherence. In atom-based applications, single-frequency lasers should also be continuously tuned to precisely match their wavelengths with the transition lines of the corresponding atoms. Continuous frequency tuning of the laser is mainly achieved by continuously scanning the laser cavity length after the intracavity tuning element etalon is locked to an oscillating laser mode. However, the modulation signals necessary in current etalon locking systems increase the noise of the continuously tunable lasers and in some respects limit their applications in Frontier scientific research. Moreover, the obtained continuous frequency tuning range with the etalon locking technique is restricted by the free spectrum range of the adopted etalon. In this paper, we systematically summarize recent progress of the continuously tunable single-frequency CW lasers based on intracavity locked etalon, including the advanced etalon locking techniques and the tuning range expansion approach. As a result, the low noise and high stable all-solid-state single-frequency CW tunable lasers are successfully developed.

KEYWORDS

all-solid-state laser, single-frequency CW laser, wideband continuous frequency tuning, high-power, stable SLM operation

1 Introduction

All-solid-state single-frequency continuous-wave (CW) lasers have intrinsic merits of high beam quality, low noise, narrow linewidth, and high coherence [1], which have been widely applied in many fields of scientific research, such as quantum optics and quantum information [2, 3], cold atom physics [4], precision measurement [5], high resolution spectroscopy [6, 7], and so on. In particular, single-frequency CW lasers with specific

wavelengths are of great interest for atom- or molecule-based applications, for example, the 455.5 nm, 852 nm and 895 nm laser corresponding to the cesium atom (Cs), 532 nm laser corresponding to the iodine molecule (I_2), 589 nm laser corresponding to the sodium atom (Na), 671 nm laser corresponding to the lithium atom (Li), 729 nm laser corresponding to the calcium atom (Ca), 767 nm and 770 nm laser corresponding to the potassium atom (K), 780 nm and 795 nm laser corresponding to the rubidium atom (Rb). To satisfy the requirements of the atom- or molecule-based applications, a single-frequency CW laser with broadband mode-hop-free continuous frequency tuning is desired, such that the laser wavelength can be continuously modified to precisely match with the absorption lines of the atoms or molecules. On the other hand, the broadband mode-hop-free continuous frequency tuning is also essential for a high-power single-frequency CW laser to guarantee its long-term stable single-longitudinal-mode (SLM) operation and enhance its adaptation to the application environment. Due to the thermal effect is extremely severe and the mode competition is fierce in the high-power single-frequency CW laser, in the same time its frequency will drift with the temperature fluctuation and air flow of the ambient environment under long-term operation, the multi-longitudinal-mode (MLM) oscillation or mode-hopping of the laser is very easy to happen [8]. Nevertheless, once the broadband continuous frequency tuning capability is equipped in a high-power single-frequency CW laser, the same one oscillating laser mode is always selected within the broadband tuning range and the other non-lasing modes are suppressed, thus ensuring that the oscillating laser mode remains oscillating in the tuning range and the mode-hop is suppressed. In this way, MLM and mode-hopping phenomena in long-term operation of the laser can hardly occur when its frequency drift does not exceed the continuous frequency tuning range, and the long-term stability of the SLM operation for the high-power laser is enhanced.

The wideband continuous frequency tuning is easily realized in a microchip designed solid-state laser [9–14] where the laser resonator length is short enough and its free spectrum range (FSR) is close to or wider than the gain bandwidth of the laser medium. In this case, only one laser mode can be oscillated, and its frequency can be continuously tuned with the tuning range close to the gain bandwidth of the laser medium (>100 GHz) by scanning the laser resonator length. However, the short resonator length results in a relative lower laser gain and the laser output power is restricted within watt level. In order to scale the laser power up to watt level, a power amplifier system, such as a master oscillator power amplifier (MOPA) [13], is necessary. For a high-power all-solid-state single-frequency CW laser, an etalon is typically used as a mode selector in the laser resonator to enforce a stable SLM operation of the laser. By varying the incident angle, temperature, or refractive index of the etalon to vary its effective optical path, the laser frequency tuning can be

implemented. In 1992, [15]. Obtained a tunable single-frequency laser with tuning range over 60 GHz by rotating the incident angle of etalon. In 2010, [16]. Realized a tunable single-frequency 671 nm laser with a tuning range of 1.5 nm, also by rotating the incident angle of a thinner etalon. In 2008 and 2013, our group demonstrated a tunable single-frequency 1,064 nm laser with tuning range of 17.2 GHz by scanning the voltage of electro-optic etalon (EOE) [17] and a tunable high-power single-frequency 532 nm laser with tuning range over 24 GHz by scanning the temperature of etalon [18], respectively. Nevertheless, the above mentioned frequency tuning of the laser is not continuous due to the laser mode hopping. By scanning the resonator length, the laser frequency can be continuously scanned within one FSR of the laser resonator, which in general is a few hundred megahertz. However, for the atom- or molecule-based experimental systems, the continuously tunable lasers with frequency tuning ranges larger than a few or a few tens of gigahertz are desired. For this purpose, the transmission peak of the etalon has to be locked to the oscillating laser mode so that it can be synchronized with the laser mode when the laser resonator length is continuously scanned [19–24]. To this end, a phase-lock loop is generally utilized in the laser system where a modulation signal is required to modulate the intracavity laser intensity and extract the error signal. The modulation signal is usually coupled into the laser system through a PZT [21, 22] or a galvanometer scanner (GS) [23] and the frequency of the modulation signal is limited in a low frequency region, hundreds of hertz to tens of kilohertz. This modulation signal increases the intensity and frequency noises of the laser at the corresponding frequency range, which restricts the laser application in the fields of precision measurement and quantum information to some extent [25–28]. In order to reduce or eliminate the influence of the modulation noise, some advanced etalon locking techniques should be explored for low-noise continuously tunable single-frequency CW lasers. In 2001, [29]. Realized a tunable single-mode quasi-continuous-wave Ti:sapphire laser with an intracavity locked EOE with a 266 kHz modulation signal in the locking system. In 2017, [30]. Presented a continuously tunable single-frequency 1,064 nm laser with fast frequency tuning of 2.40 THz/s by using an EOE made by $RbTiOPO_4$ (RTP) crystal in laser resonator, and the continuous frequency tuning of 6 GHz [30] and 14 GHz [31] were achieved, respectively. Moreover, [32]. First realized a stable single-frequency operation of a semiconductor laser by utilizing an intracavity stabilized birefringent etalon (BE) in 2004 [33], where the modulation signal was not necessary and the locking signal was obtained by analyzing the polarization of the reflection from the etalon. These studies paved an effective and feasible reference to develop a low-noise single-frequency CW tunable laser. On this basis, low-noise high-power continuously tunable single-frequency CW Ti:sapphire lasers with intensity noise manipulation [34] and modulation-noise-free [35] were realized respectively. In addition, the continuous laser frequency tuning range obtained with the etalon locking

technique is confined within the FSR of the etalon. In 2015, Radnatarov *et al.* [23] achieved a quasi-continuously frequency tunable 532 nm laser with a tuning range of 240 GHz by locking two etalons with different thickness and automatically stitching several smooth frequency scanning ranges (18 GHz @532 nm) [23], which gave out an ingenious method to realize broadband continuously tunable lasers. On further investigation, it was found that the continuous tuning limit of the etalon can be broken by deliberately introducing a nonlinear loss into the laser resonator. It was proved that the nonlinear loss of the lasing mode was half of that of the non-lasing mode and the non-lasing mode can be absolutely inhibited [36–40]. Under the introduced nonlinear losses, mode-hop-free continuous tuning was achieved for the 532 nm laser up to 80 GHz [36] and for the 795 nm laser up to 48 GHz [41], as well as for other continuously tunable lasers [42–46]. The continuous tuning range of these lasers was determined by their effective gain bandwidth and nonlinear losses. However, by combining the technique of intracavity locked etalon with the introduced nonlinear loss, the continuous frequency tuning of a single-frequency CW laser could be effectively expanded beyond the FSR of the utilized etalon, and broadband continuously tunable all-solid-state single-frequency CW 1,064/532 nm dual-wavelength laser [47] and 1,080/540 dual-wavelength laser [48] were successfully realized. The obtained continuous frequency tuning ranges for the high-power 532 nm and 540 nm lasers were 222.4 GHz and 314.04 GHz, respectively, which were, to the best of our knowledge, the broadest continuum tuning ranges at their respective wavelengths achieved by simply scanning the laser resonator length.

2 Low noise continuously tunable all-solid-state single-frequency continuous-wave Ti:Sapphire lasers with advanced etalon locking techniques

2.1 Electro-optic etalon locking

For an all-solid-state single-frequency CW Ti:sapphire laser, an etalon is often inserted into the laser resonator to finely select a oscillating laser mode and then keep SLM laser operation. In order to realize continuous laser frequency tuning, the transmission peak of the etalon obliges to be locked onto the oscillating laser mode [22, 49–51]. So far, a PZT-driven etalon is the most popular candidate to achieve this goal. For the PZT-driven etalon, the modulation signal is coupled into the laser system through the used PZT and the frequency of the modulation signal is required to match with the mechanical resonance frequency of the PZT to obtain a well-defined error signal for stable etalon locking. This modulation signal with constant frequency increases both the laser intensity and the

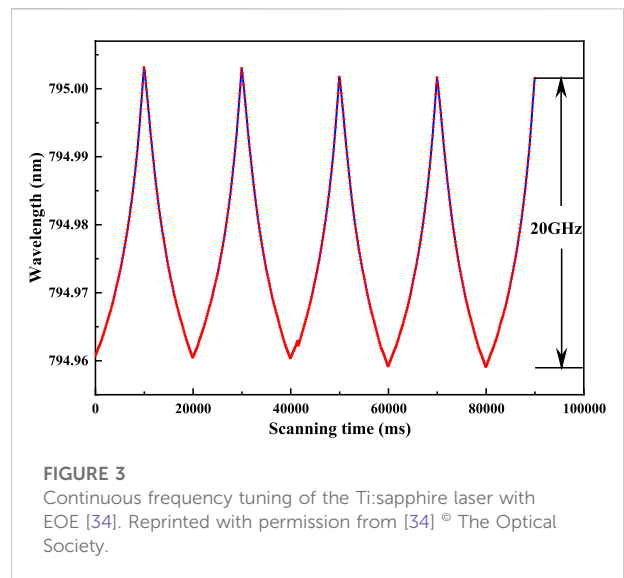
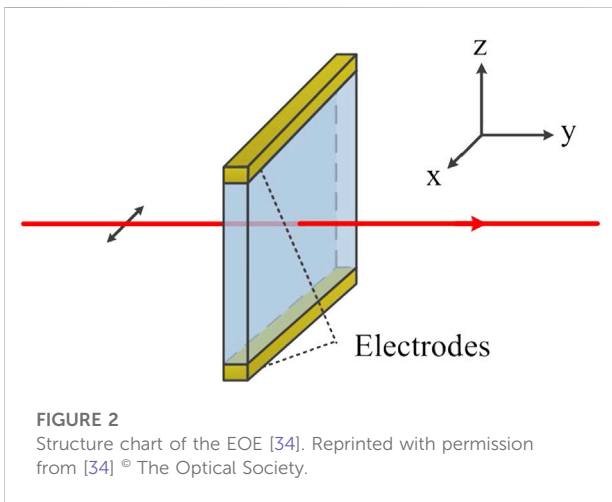
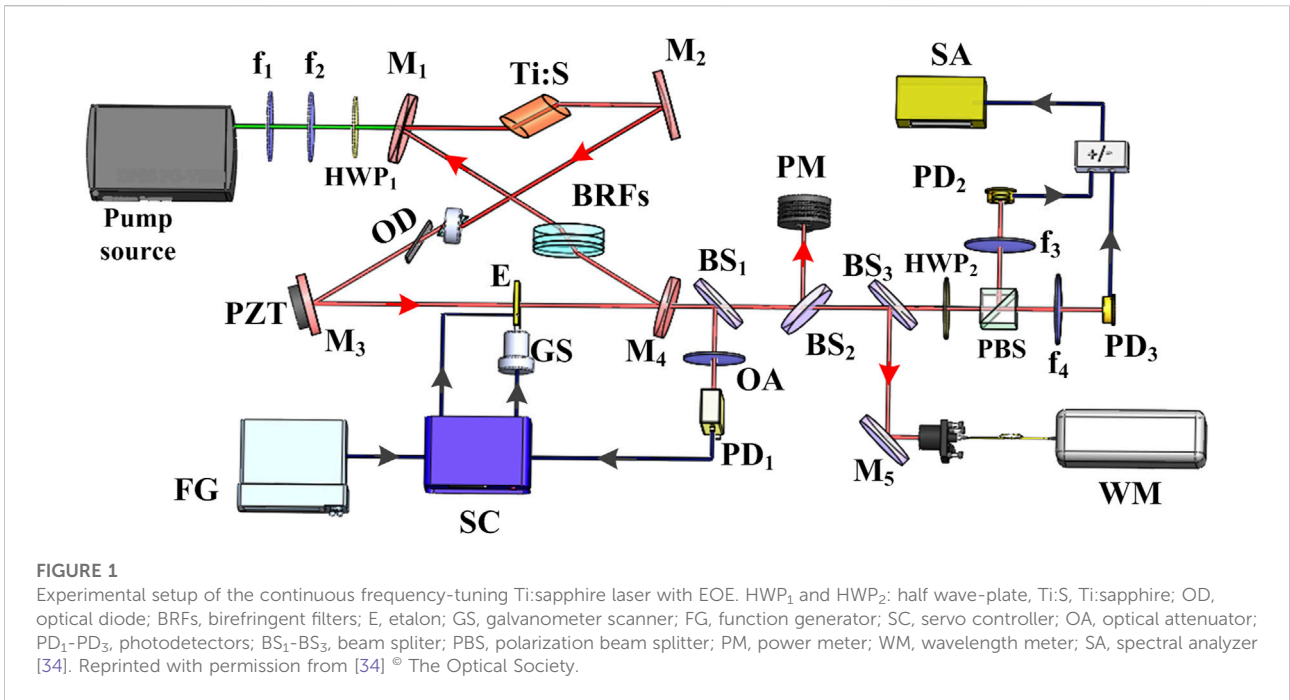
frequency noise at the corresponding analysis frequency. To overcome this deficiency, an etalon made of an electro-optic crystal can be chosen to act as a fine mode selector and tuner in a continuously tunable Ti:sapphire laser, and the modulation signal can be coupled into the laser system *via* the electro-optic effect of the crystal. Owing to the electro-optic effect of the crystal is independent of the signal frequency, the modulation frequency can be chosen arbitrarily [34].

In the all-solid-state single-frequency CW tunable Ti:sapphire laser as shown in Figure 1, an EOE made by lithium niobate (LiNbO₃) crystal was inserted into the laser resonator [34]. The dimension of the utilized EOE was 10 mm × 1 mm × 5 mm (X × Y × Z) with its optical axis along the z axis, as shown in Figure 2. The transmission surface of the crystal was uncoated and polished. The incident laser beam propagated through the crystal with its polarization orientation aligned with the crystal's x-axis. The modulation signal was supplied to the electrodes to generate a modulated electric field in the crystal along its optical axis, which was then used to generate a modulation of the intracavity laser intensity. With the feedback-lock loop that is same as the usual phase-locking systems [22, 23], the EOE could be stably locked. When the EOE was locked to the oscillation wavelength of 795.0046 nm with six different modulation frequencies (32 kHz, 50 kHz, 84 kHz, 100 kHz, 123 kHz, and 150 kHz), the continuous laser frequency tuning ranges of larger than 20 GHz were all obtained as shown in Figure 3, which demonstrated that the modulation frequency used in the process of EOE locking did not influence the continuous frequency tuning property of the Ti:sapphire laser.

In the case of changing the modulation frequency to realize the continuous frequency tuning of the Ti:sapphire laser, its intensity noise was successfully manipulated as shown in Figure 4. After the modulation frequency of the EOE locking system was modified, the harmful intensity noise bump caused by the modulation signal was shifted with the variation of the modulation frequency. In order to eliminate the influence of the modulation signal on the intensity noise and expand the application of the presented Ti:sapphire laser, the modulation frequency of the EOE could be chosen beyond some interesting frequency range, which was the prominent advantage of the EOE locking technique compared with the PZT-based etalon locking system. On the other hand, the modulation signal with higher frequency could be easily selected for the EOE, which was helpful for increasing the signal-to-noise ratio of the error signal and then enhancing the stability of the etalon locking [52].

2.2 Birefringent etalon locking

Although the intensity noise of the continuously tunable Ti:sapphire laser with the intracavity locked EOE can be manipulated, the modulation signal still exists in the laser system and increases the laser noise. In order to thoroughly



eliminate the influence of the modulation signal on the laser noise and obtain a low-noise single-frequency CW Ti:sapphire laser to satisfy the requirements of quantum information and precise measurement, an etalon made of a birefringent crystal can be adopted in the laser system. With the assistance of the birefringent effect of the crystal, the error signal can be extracted by detecting the polarization state variation of the reflected laser from the etalon and the etalon locking can be implemented by a modulation-free locking system [35].

For a BE as shown in Figure 5, the optical axis and transmission surface of the crystal are in the direction of z -axis and x - o - z plane, respectively. When a linear polarized laser passes through the BE along its y -axis and the polarization orientation of the laser is rotated by a small angle θ ($2 \sim 3^\circ$) relative to the crystal's x -axis, the incident laser (E_0) will decompose into two components in the crystal, the major one E_1 along x -axis and the minor one E_2 along z -axis. According to

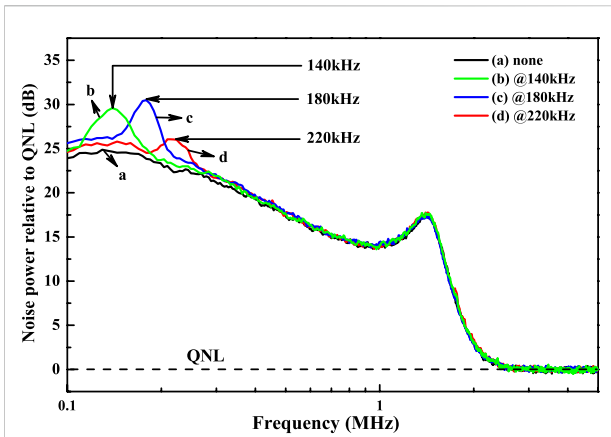


FIGURE 4 Intensity noise of the Ti:sapphire laser with EOE at different modulation frequencies. (a) Without modulation signal, (b) at 140 kHz, (c) at 180 kHz, (d) at 220 kHz [34]. Reprinted with permission from [34] © The Optical Society.

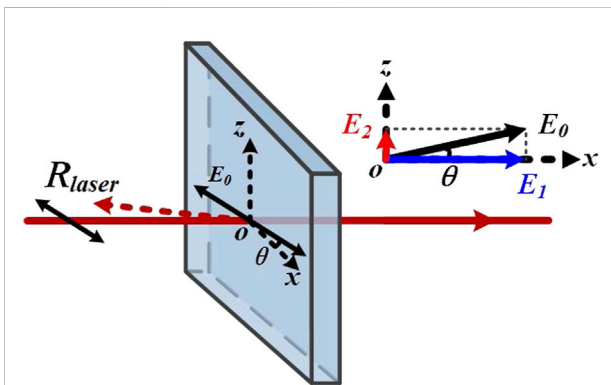


FIGURE 5 Structure chart of the BE [35]. © [2022] IEEE. Reprinted, with permission, from [35].

the birefringence and reflection properties of the etalon, the polarization property of the reflected laser from the etalon (R_{laser}) is varied when the laser frequency is resonant with the etalon or not. When the major one laser component E_1 is resonant with the etalon, its reflection coefficient equals zero, and the reflected laser is linearly polarized along z -axis (only E_2 component can be reflected). However, when it is mismatched with the etalon, the reflected laser is elliptically polarized with different helicity [32]. The error signal used to feedback lock the BE can be extracted by detecting this different polarization state of R_{laser} through a combiner consisting of a quarter-wave plate and a polarization beam splitter (PBS). When the laser frequency is resonant with the etalon, the error signal equals zero. Otherwise, the error signal will have a non-zero value and its

sign is determined by the frequency difference between the laser and the resonance point of the BE. With this error signal, the BE can be stably feedback locked to the oscillating laser mode. The modulation signal is unnecessary in this locking system and the modulation-free BE locking is implemented.

In the continuously tunable single-frequency CW Ti:sapphire laser as shown in Figure 6, a BE made by LiNbO_3 crystal was adopted as the mode selector [35]. It was inserted into the laser resonator with its x -axis setting about $2 \sim 3^\circ$ relative to the polarization orientation of the oscillating light and stably locked to an oscillating laser mode by detecting the polarization state of the reflected laser from it. After the BE was locked, the continuous laser frequency tuning with the range larger than 40 GHz at the whole tuning range of 700–1,000 nm was achieved. On this basis, the noise properties of the continuously tunable single-frequency CW Ti:sapphire lasers with PZT-driven etalon, EOE, and BE were compared as shown in Figures 7, 8. The comparison results obviously revealed that the influences of the extra modulation signal on the intensity as well as the frequency noises were both vanished once the BE and modulation-free locking method were adopted in the Ti:sapphire laser, which resulted from that the modulation signal was unnecessary in the BE locking system and there were no modulation noises imprinted in laser intensity and frequency noises. Eventually, a modulation-noise-free continuously tunable single-frequency CW Ti:sapphire laser was successfully attained. The obtained low-noise continuously tunable single-frequency CW Ti:sapphire laser could be well used in the research fields of quantum-enhanced precision measurement, quantum information network and cold-atom physics.

3 Expanding the continuous laser frequency tuning range by combining the intracavity locked etalon with nonlinear loss

As mentioned above, an etalon is often utilized in a single-frequency laser to narrow its gain linewidth and keep the SLM laser operation. After the transmission peak of the etalon is locked to the oscillating laser mode and the laser resonator length is continuously scanned, the continuous laser frequency tuning can be realized only within one FSR of the etalon. The laser mode hopping between two adjacent transmission peaks of the etalon occurs when the laser frequency is continuously tuned to the edge of the FSR of the etalon around the central wavelength of laser medium. However, when a nonlinear loss is deliberately introduced into a laser resonator with locked etalon, the laser frequency can be continuously tuned beyond the tuning edge of the etalon, owing to the nonlinear loss of non-oscillating mode is twice that of the oscillating mode and the mode-hopping at the tuning edge of the etalon is effectively suppressed. As a result, the continuous frequency tuning range of the single-frequency CW

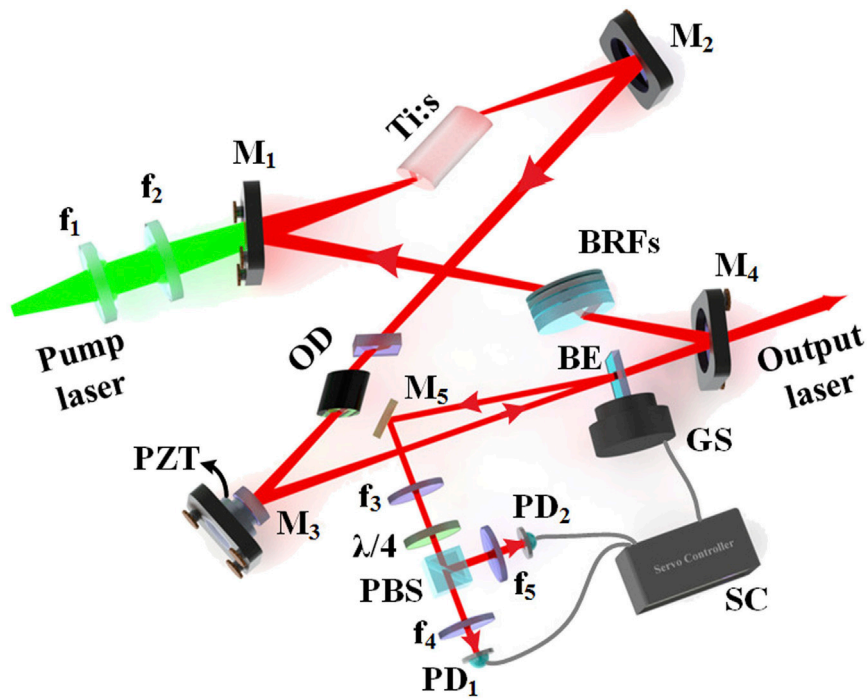


FIGURE 6 Experimental setup of the continuous frequency-tuning laser with intravity-locked BE. Ti:S, Ti:Sapphire; OD, optical diode; BRFs, birefringent filters; BE, birefringent etalon; GS, galvanometer scanner; SC, servo controller; PZT, piezoelectric transducer; PBS, polarization beam splitter; PD₁-PD₂, photodetectors; M₁-M₅, mirrors; f₁-f₅, lenses [35]. © [2022] IEEE. Reprinted, with permission, from [35].

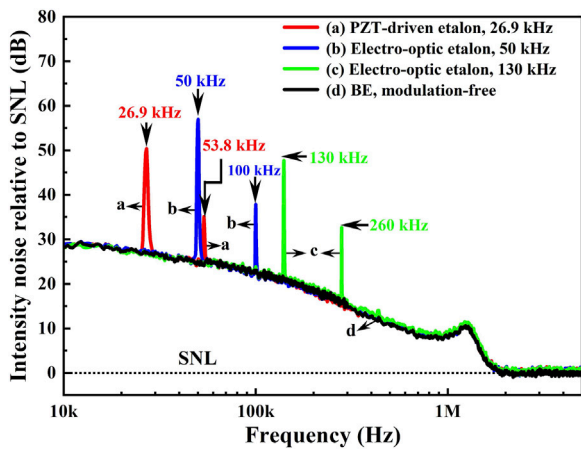


FIGURE 7 Intensity noises of the Ti:S lasers with (a) PZT-driven etalon with the modulation frequency of 26.9 kHz, red curve; (b) electro-optic etalon with the modulation frequency of 50 kHz, blue curve; (c) electro-optic etalon with the modulation frequency of 130 kHz, green curve; (d) BE with modulation-free, black curve [35]. © [2022] IEEE. Reprinted, with permission, from [35].

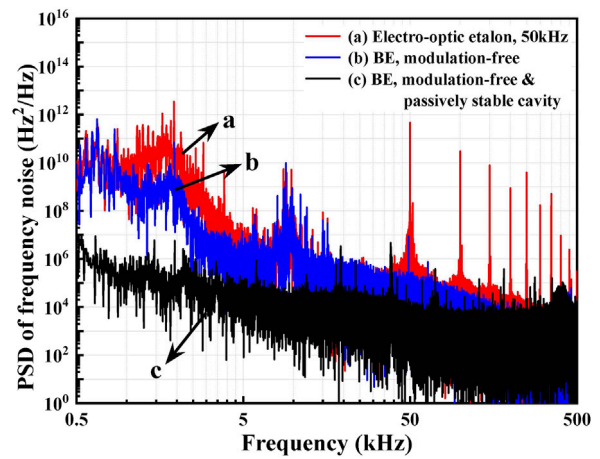


FIGURE 8 Frequency noises of the Ti:S lasers with (a) electro-optic etalon with the modulation frequency of 50 kHz, red curve; (b) BE with modulation-free, blue curve; (c) BE with modulation-free and in a passively stable cavity, black curve [35]. © [2022] IEEE. Reprinted, with permission, from [35].

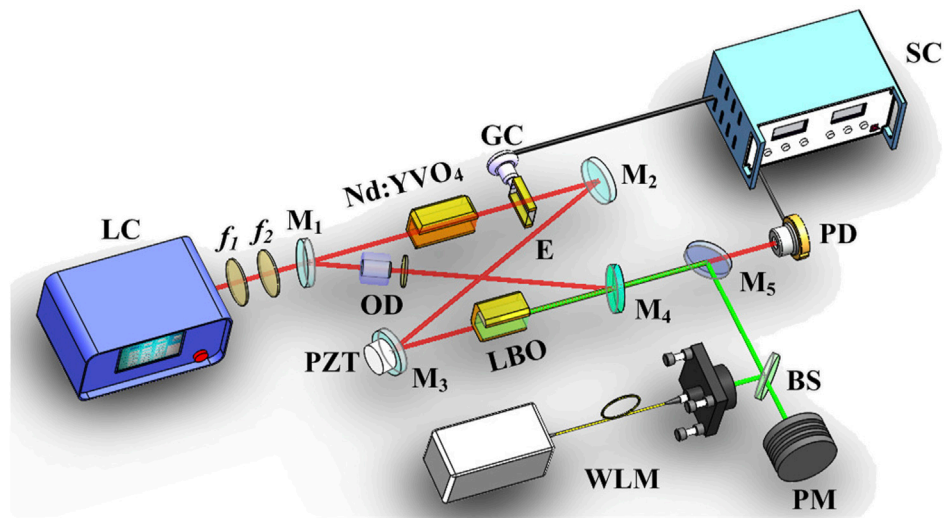


FIGURE 9

Schematic diagram of super broadband tunable CW single-frequency 1,064/532 nm laser. LC, laser controller; f_{1-2} , lenses; M_{1-4} , mirrors; Nd:YVO₄, Nd³⁺-doped yttrium vanadate; LBO, lithium triborate; E, etalon; GC, galvanometer scanner; SC, servo controller; OD, optical diode; PZT, piezoelectric transducer; PD, photodetector; BS, beam splitter; PM, power meter; WLM, wavelength meter [47]. © [2022] IEEE. Reprinted, with permission, from [47].

laser is effectively extended beyond the FSR of the etalon, and the maximal continuous frequency tuning range of the laser can be expressed as [47],

$$\Delta\nu_{\max} = \nu_{\text{FSR}} + \frac{\left(\frac{\Delta\nu_H}{2}\right)^2}{\nu_{\text{FSR}}} \times \frac{\eta}{\eta + L} \quad (1)$$

where ν_{FSR} is the FSR of the etalon, $\Delta\nu_H$ is the gain bandwidth of laser gain medium, L is the linear loss in the laser cavity, and η is the nonlinear second harmonic (SH) conversion efficiency. With this tuning range extension technique, the continuously tunable single-frequency CW dual-wavelength 1,064/532 nm and 1,080/540 nm lasers with broadband tuning range have been obtained.

3.1 Continuously tunable single-frequency continuous-wave dual-wavelength 1,064/532 nm laser

The wideband continuous frequency tuning of the 1,064/532 nm dual-wavelength laser was achieved in an all-solid-state single-frequency CW intracavity frequency-doubled Nd:YVO₄/LBO laser as shown in Figure 9 [47]. An EOE was inserted into the laser resonator and the LBO crystal was used as a nonlinear frequency-doubled crystal to introduce a nonlinear loss. In this laser, the FSR of the etalon was 59 GHz, the gain bandwidth of laser gain medium was 255 GHz, the intracavity linear loss was 5.8%, and the SH conversion efficiency was 1.87%. According to the Eq. (1), the maximal continuous frequency tuning range of

126.18 GHz and 252.36 GHz for the 1,064 nm and 532 nm lasers were calculated, respectively. In experiment, after the EOE was locked to the oscillating laser mode and the resonator length was continuously scanned, the continuous tunable 532 nm laser with the maximal tuning range of 222.4 GHz was achieved as shown in Figure 10A. The experimental result was consistent with the theoretical calculation. In the same time, the effectivity of the present method was further verified by replacing the high-reflection coated mirror M_2 with another plane mirror coated with partial transmission film at 1,064 nm with the transmission of 4%. In this case, the intracavity linear loss and the SH conversion efficiency were modified to 9.8% and 1.2% respectively. According to Eq. (1), the maximal continuous tuning range of 178.12 GHz for the 532 nm laser could be attained. In experiment, after the EOE was locked, the maximal continuous frequency tuning range of 154 GHz at 532 nm was implemented as shown in Figure 10B, which distinctly notarized the expansion ability of the nonlinear loss on the continuous tuning range of the single-frequency CW laser.

3.2 Continuously tunable single-frequency continuous-wave dual-wavelength 1,080/540 nm laser with high output power and long-term stable single-logitudinal-mode operation

The continuously tunable single-frequency CW dual-wavelength 1,080/540 nm laser was achieved in an

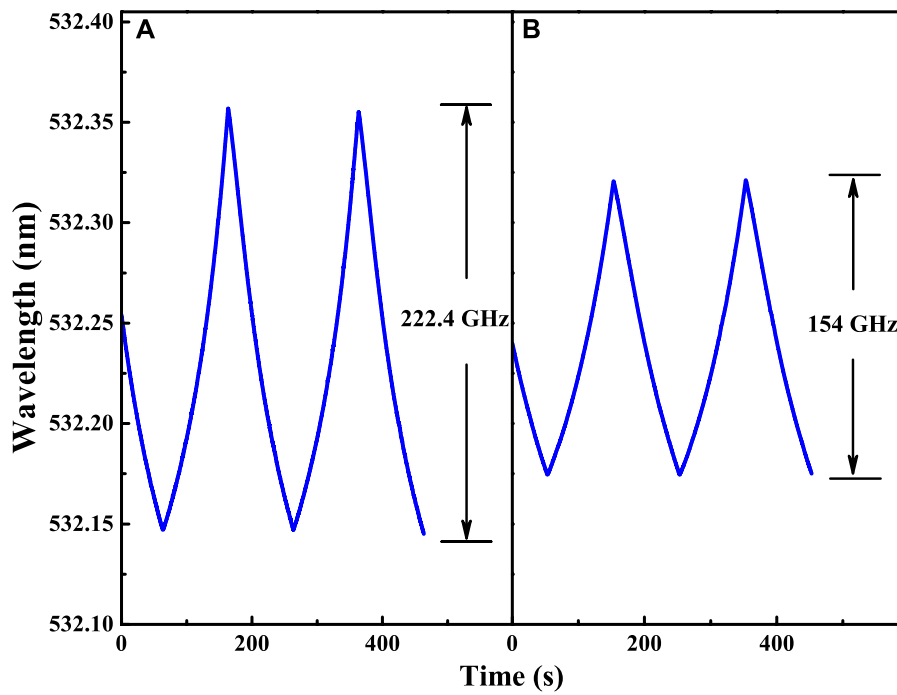


FIGURE 10
 The continuous tuning range of the CW single-frequency 532 nm laser combining the locked EOE and nonlinear loss with different L and η : (A) $L = 5.8\%$ and $\eta = 1.87\%$, (B) $L = 9.8\%$ and $\eta = 1.2\%$ [47]. © [2022] IEEE. Reprinted, with permission, from [47].

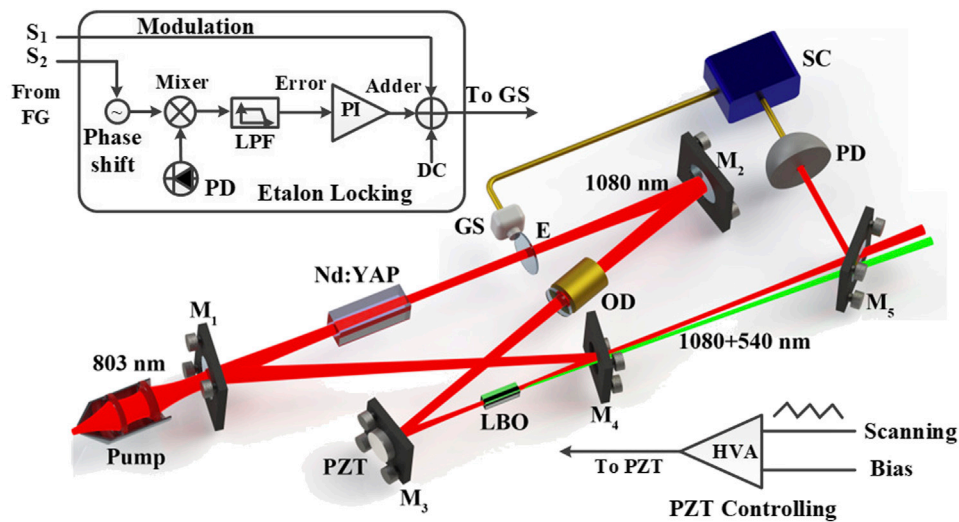
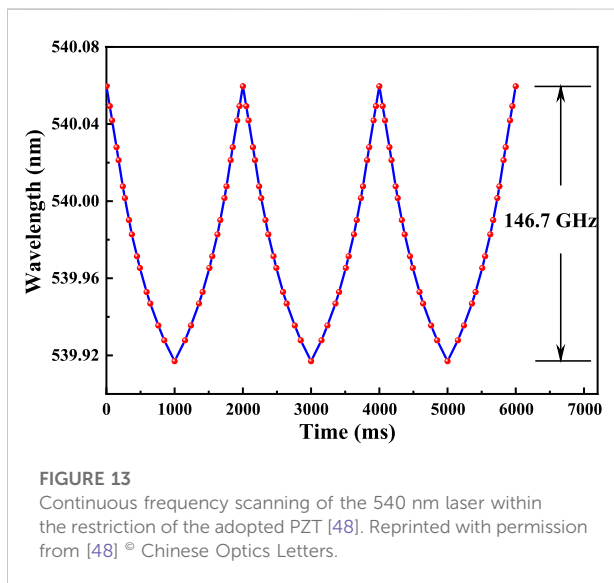
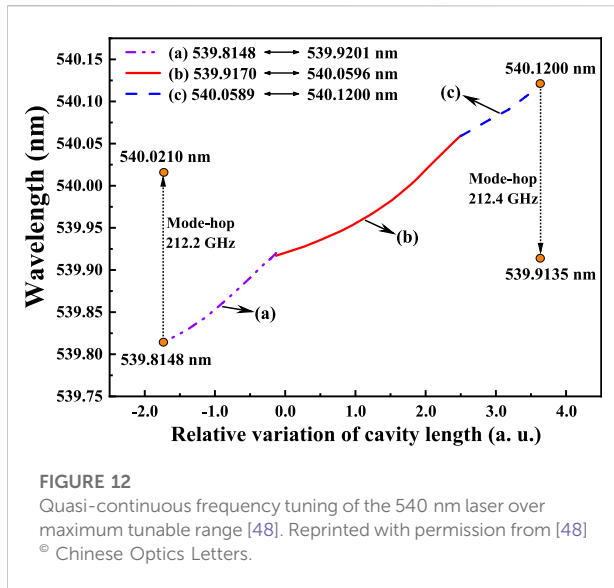


FIGURE 11
 Experimental setup of the continuously tunable high-power single-frequency CW 1080/540 nm dual-wavelength laser. Nd:YAP, Nd:YAlO₃; GS, galvanometer scanner; E, etalon; SC, servo controller; OD, optical diode; PZT, piezoelectric transducer; LBO, lithium triborate; PD, photodetector; M₁₋₅, mirrors; FG, function generator; LPF, low pass filter; PI, proportion and integration; DC, direct current; HVA, high voltage amplifier [48]. Reprinted with permission from [48] © Chinese Optics Letters.



intracavity frequency-doubled high-power Nd:YAP/LBO laser [48], as shown in Figure 11. In this high-power single-frequency CW laser, the gain competition was fierce owing to the high gain and severe thermal effect of the laser crystal. In order to obtain SLM operation and high output power of the laser in the tuning process, an uncoated quartz etalon with the thickness of 0.8 mm and the bandwidth of 148.92 GHz was designed and adopted in the laser resonator. The LBO crystal converted the 1,080 nm laser into a frequency-doubled 540 nm laser and simultaneously introduced a nonlinear loss. In experiment, the maximal

output powers of the single-frequency 1,080 and 540 nm lasers were 2.39 and 4.18 W respectively. After the etalon was feedback locked to the oscillating laser mode and the laser resonator length was continuously scanned, the continuously tunable high-power 1,080/540 nm dual-wavelength laser with the potential continuous tuning range of 314.04 GHz at 540 nm was achieved as shown in Figure 12, which was consistent with the theoretically calculated value of 334.44 GHz. In reality, restricted by the finite displacement of the PZT used in the laser system, the continuous frequency tuning range of 146.7 GHz was experimentally obtained, as shown in Figure 13. If the variation of the resonator length was large enough the maximal continuous frequency tuning range of 314.03 GHz could be really achieved.

The obtained broadband continuous frequency tuning capability could also enhance the stability of the long-term SLM operation of the high-power laser and its adaptation to the ambient environment. The whole optical elements in the laser resonator were mounted in a duralumin monoblock construction. Considering the optical cavity length of the laser and the thermal expansion coefficient of the duralumin materials, the continuous frequency scanning range of 314.03 GHz for the 540 nm laser corresponded to the ambient temperature fluctuation of $\pm 12^\circ\text{C}$, which meant that the obtained high-power 1,080/540 nm laser could maintain stable SLM operation in long-term running in a common laboratory where the environment temperature fluctuation was generally less than $\pm 12^\circ\text{C}$. In a word, when the locked etalon and nonlinear loss were simultaneously introduced into the high-power Nd:YAP/LBO laser, the wideband continuous laser frequency tuning and long-term stable SLM laser operation were successfully realized. The experimental results revealed that by combining the intracavity locked etalon and nonlinear loss, the continuous frequency tuning range of single-frequency CW lasers could be effectively expanded, and a continuously tunable single-frequency CW laser with broadband tuning range and long-term stable SLM operation could be simultaneously realized.

4 Conclusion

With the rapid development of the scientific research of cold atom physics, high-resolution spectroscopy and so on, the continuously tunable all-solid-state single-frequency CW lasers have attracted increasing interest of the community. Currently, various advances have been made in the continuously tunable single-frequency CW lasers, including the advanced etalon locking techniques and the tuning range expansion approach. Adopting an intracavity locked EOE in the laser resonator, a tunable single-frequency CW Ti:

sapphire laser with intensity noise manipulation was obtained. In this laser system, the electro-optic effect of the EOE was utilized to modulate the intracavity laser intensity and the laser intensity noise was manipulated by changing the modulation frequency, which overcame the defect of the tunable Ti:sapphire laser with a PZT-driven etalon whose modulation noise was fixed at a constant frequency. However, the modulation noise still existed in the tunable Ti:sapphire laser with an EOE. To eliminate the modulation noise in the laser system, a locked BE with modulation-free locking method was employed in the tunable Ti:sapphire laser and a modulation-noise-free continuously tunable single-frequency CW Ti:sapphire laser was successfully achieved. Based on this, the continuous frequency tuning range of tunable single-frequency CW lasers can be effectively extended by combining the intracavity locking etalon with an introduced nonlinear loss. Depending on this approach, the continuously tunable single-frequency CW lasers with broadband tuning ranges and long-term stable SLM operation were realized. The presented continuous frequency tuning techniques paved a good way to develop different kinds of continuously tunable single-frequency CW lasers with broadband tuning range and kinds of high-power single-frequency CW lasers with long-term stable SLM operation. Based on these techniques, low-noise and high-stable all-solid-state single-frequency CW lasers have been developed [34, 35, 47, 48, 53–55] to satisfy the requirement of the Frontier scientific research [56–58]. With the assistance of the sum-frequency conversion [59], stimulated raman scattering (SRS) [60], and optical parametric oscillation (OPO) [61] technologies, the wavelength of the obtained continuously tunable laser can be further extended to cover the spectral region from the deep ultraviolet to the middle-infrared.

References

1. Wang Y, Tian Y, Sun X, Tian L, Zheng Y. Noise transfer of pump field noise with analysis frequency in a broadband parametric downconversion process. *Chin Opt Lett* (2021) 19:052703. doi:10.3788/COL202119.052703
2. Kimble HJ. The quantum internet. *Nature* (2008) 453:1023–30. doi:10.1038/nature07127
3. Huo M, Qin J, Cheng J, Yan Z, Qin Z, Su X, et al. Deterministic quantum teleportation through fiber channels. *Sci Adv* (2018) 4:eaas9401. doi:10.1126/sciadv.aas9401
4. Kuwamoto T, Honda K, Takahashi Y, Yabuzaki T. Magneto-optical trapping of Yb atoms using an inter combination transition. *Phys Rev A (Coll Park)* (1999) 60: R745–8. doi:10.1103/PhysRevA.60.R745
5. Li BB, Bilek J, Hoff UB, Madsen LS, Forstner S, Prakash V, et al. Quantum enhanced optomechanical magnetometry. *Optica* (2018) 5:850–6. doi:10.1364/OPTICA.5.000850
6. Vassen W, Zimmermann C, Kallenbach R, Hänsch TW. A frequency-stabilized titanium sapphire laser for high-resolution spectroscopy. *Opt Commun* (1990) 75: 435–40. doi:10.1016/0030-4018(90)90209-C
7. Markov BN, Babin SA, Blaszcak Z, Gangrsky YP, Kobtsev SM, Penionzhkevich YE. High-resolution laser spectrometer for fundamental and

Author contributions

PJ: Investigation, Writing-original draft preparation. JW, Investigation. JS, Writing-review and editing. HL, Conceptualization, Writing-review and editing. KP, Conceptualization, Supervision. All authors have read and agreed to the published version of the manuscript.

Funding

This study was supported by the National Natural Science Foundation of China (62105192, 61975100, and 62027821); Applied Basic Research Program of Shanxi Province (20210302121004); Program for the Innovative Talents of High Education Institutions of Shanxi; Fund for Shanxi “1,331 Project” Key Subjects Construction.

Conflict of interest

The authors declare that the research was conducted in the absence of any commercial or financial relationships that could be construed as a potential conflict of interest.

Publisher's note

All claims expressed in this article are solely those of the authors and do not necessarily represent those of their affiliated organizations, or those of the publisher, the editors and the reviewers. Any product that may be evaluated in this article, or claim that may be made by its manufacturer, is not guaranteed or endorsed by the publisher.

applied research. *Bull Russ Acad Sci Phys* (2007) 71:844–7. doi:10.3103/S1062873807060184

8. Peng W, Jin P, Li F, Su J, Lu H, Peng K. A review of the high-power all-solid-state single-frequency continuous-wave laser. *Micromachines* (2021) 12:1426. doi:10.3390/mi12111426

9. Gavrilović P, Singh S, Smirnitkii VB, Bisberg J, O'Neil M. High-power grating tuned semiconductor diode lasers and single-frequency diode-pumped Nd:YAG microcavity lasers. *AIP Conf Proc* (1991) 240:37–48. doi:10.1063/1.41382

10. Taira T, Mukai A, Nozawa Y, Kobayashi T. Single-mode oscillation of laser-diode-pumped Nd:YVO₄ microchip lasers. *Opt Lett* (1991) 16:1955–7. doi:10.1364/OL.16.001955

11. Wetter N, de Matos P, Ranieri I, Courrol L, Morato S. Single frequency, continuously tunable, diode-pumped Nd:LiY_{0.5}Gd_{0.5}F₄ microlaser. *Opt Commun* (2002) 204:311–5. doi:10.1016/S0030-4018(02)01237-3

12. Qiao Y, Zheng S, Chi H, Jin X, Zhang X. Electro-optically tunable microwave source based on composite-cavity microchip laser. *Opt Express* (2012) 20:29090–5. doi:10.1364/OE.20.029090

13. Wang X, Riesbeck T, Eichler HJ. Tunable single frequency microchip Nd:YAP MOPA laser operating at 1.08 μm . *Laser Phys* (2013) 23:045804. doi:10.1088/1054-660x/23/4/045804

14. Gui K, Zhang Z, Xing Y, Zhang H, Zhao C. Frequency difference thermally and electrically tunable dual-frequency Nd:YAG/LiTaO₃ microchip laser. *Appl Sci* (2019) 9:1969. doi:10.3390/app9101969
15. Harrison J, Finch A, Flint J, Moulton P. Broad-band rapid tuning of a single-frequency diode-pumped neodymium laser. *IEEE J Quan Electron* (1992) 28: 1123–30. doi:10.1109/3.135236
16. Camargo FA, Zanon-Willette T, Badr T, Wetter NU, Zondy JJ. Tunable single-frequency Nd:YVO₄/BiB₃O₆ ring laser at 671 nm. *IEEE J Quan Electron* (2010) 46:804–9. doi:10.1109/JQE.2009.2038496
17. Zheng Y, Lu H, Li Y, Zhang K, Peng K. Broadband and rapid tuning of an all-solid-state single-frequency Nd:YVO₄ laser. *Appl Phys B* (2008) 90:485–8. doi:10.1007/s00340-007-2889-y
18. Wang W, Lu H, Su J, Peng K. Broadband tunable single-frequency Nd:YVO₄/LBO green laser with high output power. *Appl Opt* (2013) 52:2279–85. doi:10.1364/AO.52.002279
19. Goldsborough JP. Scanning single frequency CW Dye laser techniques for high-resolution spectroscopy. *Opt Eng* (1974) 13:136523. doi:10.1117/12.7978718
20. Danielmeyer HG, Leibolt WN. Stable tunable single-frequency Nd:YAG laser. *Appl Phys (Kowloon)* (1974) 3:193–8. doi:10.1007/BF00884496
21. Kobtsev S, Baraoulya V, Lunin V. Ultra-narrow-linewidth combined CW Ti:sapphire/dye laser for atom cooling and high-precision spectroscopy. *Solid State Lasers XVI: Tech Devices* (2007) 6451:6451U. doi:10.1117/12.699241
22. Sun X, Wei J, Wang W, Lu H. Realization of a continuous frequency-tuning Ti:sapphire laser with an intracavity locked etalon. *Chin Opt Lett* (2015) 13: 071401–4. doi:10.3788/COL201513.071401
23. Radnatarov D, Kobtsev S, Khripunov S, Lunin V. 240-GHz continuously frequency-tunable Nd:YVO₄/LBO laser with two intra-cavity locked etalons. *Opt Express* (2015) 23:27322–7. doi:10.1364/OE.23.027322
24. Xu X, Li X, Yan R, Ma Y, Chen Z, Yu Y, et al. Linearly frequency-tuned LD-pumped Nd:YVO₄ laser with an 18-GHz broadband tuning range. *Appl Opt* (2017) 56:9150–5. doi:10.1364/AO.56.009150
25. Bai L, Wen X, Yang Y, He J, Wang J. Laser intensity noise suppression for preparing audio-frequency squeezed vacuum state of light. *Appl Sci* (2020) 10:1415. doi:10.3390/app10041415
26. Wen X, Han Y, Liu J, He J, Wang J. Polarization squeezing at the audio frequency band for the Rubidium D₁ line. *Opt Express* (2017) 25:20737–48. doi:10.1364/OE.25.020737
27. McKenzie K, Gray MB, Lam PK, McClelland DE. Technical limitations to homodyne detection at audio frequencies. *Appl Opt* (2007) 46:3389–95. doi:10.1364/AO.46.003389
28. Stefszky MS, Mow-Lowry CM, Chua SSS, Shaddock DA, Buchler BC, Vahlbruch H, et al. Balanced homodyne detection of optical quantum states at audio-band frequencies and below. *Class Quan Gravity* (2012) 29:145015. doi:10.1088/0264-9381/29/14/145015
29. Cabaret L, Camus P, Leroux R, Philip J. Intracavity LiNbO₃ Fabry–Perot etalon for frequency stabilization and tuning of a single-mode quasi-continuous-wave titanium:sapphire ring laser. *Opt Lett* (2001) 26:983–5. doi:10.1364/OL.26.000983
30. Xu X, Li X, Yan R, Ma Y, Dong Z, Fan R, et al. 2.4 THz/s continuously linearly frequency-modulated Nd:YVO₄ laser. *Opt Express* (2017) 25:23199–206. doi:10.1364/OE.25.023199
31. Xu X, Fan R, Li X, Ma Y, Yan R, Wang X, et al. 14 GHz broadband and continuously frequency-tuned Nd:YVO₄ laser with an RTP etalon. *Appl Opt* (2018) 57:2287–91. doi:10.1364/AO.57.002287
32. Gardner KS, Abram RH, Riis E. A birefringent etalon as single-mode selector in a laser cavity. *Opt Express* (2004) 12:2365–70. doi:10.1364/OPEX.12.002365
33. Abram RH, Gardner KS, Riis E, Ferguson AI. Narrow linewidth operation of a tunable optically pumped semiconductor laser. *Opt Express* (2004) 12:5434–9. doi:10.1364/OPEX.12.005434
34. Jin P, Lu H, Wei Y, Su J, Peng K. Single-frequency CW Ti:sapphire laser with intensity noise manipulation and continuous frequency-tuning. *Opt Lett* (2017) 42: 143–6. doi:10.1364/OL.42.000143
35. Jin P, Xie Y, Cao X, Su J, Lu H, Peng K. Modulation-noise-free continuously tunable single-frequency CW Ti:Sapphire laser with intracavity-locked birefringent etalon. *IEEE J Quan Electron* (2022) 58:1–6. doi:10.1109/JQE.2021.3137832
36. Martin KI, Clarkson WA, Hanna DC. Self-suppression of axial mode hopping by intracavity second-harmonic generation. *Opt Lett* (1997) 22:375–7. doi:10.1364/OL.22.000375
37. Greenstein S, Rosenbluh M. The influence of nonlinear spectral bandwidth on single longitudinal mode intra-cavity second harmonic generation. *Opt Commun* (2005) 248:241–8. doi:10.1016/j.optcom.2004.11.085
38. Lu H, Su J, Zheng Y, Peng K. Physical conditions of single-longitudinal-mode operation for high-power all-solid-state lasers. *Opt Lett* (2014) 39:1117–20. doi:10.1364/OL.39.001117
39. Guo Y, Lu H, Xu M, Su J, Peng K. Investigation about the influence of longitudinal-mode structure of the laser on the relative intensity noise properties. *Opt Express* (2018) 26:21108–18. doi:10.1364/OE.26.021108
40. Lu H, Peng K. Realization of the single-frequency and high power as well as frequency-tuning of the laser by manipulating the nonlinear loss. *J Quan Opt* (2015) 21:171–6. doi:10.3788/asqo20152102.0171
41. Lu H, Sun X, Wang M, Su J, Peng K. Single frequency Ti:sapphire laser with continuous frequency-tuning and low intensity noise by means of the additional intracavity nonlinear loss. *Opt Express* (2014) 22:24551–8. doi:10.1364/OE.22.024551
42. Eismann U, Bergschneider A, Sievers F, Kretzschmar N, Salomon C, Chevy F. 2.1-watts intracavity-frequency-doubled all-solid-state light source at 671 nm for laser cooling of lithium. *Opt Express* (2013) 21:9091–102. doi:10.1364/OE.21.009091
43. Murdoch KM, Clubley DA, Snadden MJ. A mode-hop-free tunable single-longitudinal-mode Nd:YVO₄ laser with 25W of power at 1064 nm. *Solid State Lasers XVIII: Tech Devices* (2009) 7193:7193P. doi:10.1117/12.809288
44. Friel GJ, Kemp AJ, Lake TK, Sinclair BD. Compact and efficient Nd:YVO₄ laser that generates a tunable single-frequency green output. *Appl Opt* (2000) 39: 4333–7. doi:10.1364/AO.39.004333
45. Okhapkin M, Skvortsov M, Belkin A, Kvashnin N, Bagayev S. Tunable single-frequency diode-pumped Nd:YAG ring laser at 1064/532 nm for optical frequency standard applications. *Opt Commun* (2002) 203:359–62. doi:10.1016/S0030-4018(02)01205-1
46. Okhapkin M, Skvortsov M, Kvashnin N, Bagayev S. Single-frequency intracavity doubled Yb:YAG ring laser. *Opt Commun* (2005) 256:347–51. doi:10.1016/j.optcom.2005.06.067
47. Jin P, Lu H, Yin Q, Su J, Peng K. Expanding continuous tuning range of a CW single-frequency laser by combining an intracavity etalon with a nonlinear loss. *IEEE J Sel Top Quan Electron* (2018) 24:1–5. doi:10.1109/JSTQE.2017.2781133
48. Jin P, Cui Y, Su J, Lu H, Peng K. Continuously tunable CW single-frequency Nd:YAP/LBO laser with dual-wavelength output. *Chin Opt Lett* (2023) 21:021403. doi:10.3788/COL202321.021403
49. [Dataset] Spectra-Physics. Matisse® 2 ultra-narrow linewidth tunable ring lasers (2022). Available: <https://www.spectra-physics.com/en/f/matisse-2-tunable-ring-laser> (Accessed August 25, 2022).
50. [Dataset] M Squared. Ultra narrow linewidth, CW Ti:sapphire laser (2022). Available: <https://www.m2lasers.com/solstis.html> (Accessed August 25, 2022).
51. [Dataset] TekhnoScan Laser Systems. CW single-frequency ring Ti:Sapphire lasers (2022). Available: http://www.tekhnoscan.com/english/ring_lasers.htm (Accessed August 25, 2022).
52. Sonnenschein V, Tomita H. A hybrid self-seeded Ti:sapphire laser with a pumping scheme based on spectral beam combination of continuous wave diode and pulsed DPSS lasers. *Appl Sci* (2022) 12:4727. doi:10.3390/app12094727
53. Li F, Zhao B, Wei J, Jin P, Lu H, Peng K. Continuously tunable single-frequency 455 nm blue laser for high-state excitation transition of cesium. *Opt Lett* (2019) 44:3785–8. doi:10.1364/OL.44.003785
54. Wei J, Cao X, Jin P, Su J, Lu H, Peng K. Diving angle optimization of BRFF in a single-frequency continuous-wave wideband tunable titanium:sapphire laser. *Opt Express* (2021) 29:6714–25. doi:10.1364/OE.419580
55. Yang H, Jin P, Su J, Xu X, Xu J, Lu H. Realization of a continuous-wave single-frequency tunable Nd:CYA laser. *Chin Opt Lett* (2022) 20:031403. doi:10.3788/COL202220.031403
56. Zhang M, Kang H, Wang M, Xu F, Su X, Peng K. Quantifying quantum coherence of optical cat states. *Photon Res* (2021) 9:887–92. doi:10.1364/PRJ.418417
57. Liu S, Han D, Wang N, Xiang Y, Sun F, Wang M, et al. Experimental demonstration of remotely creating wigner negativity via quantum steering. *Phys Rev Lett* (2022) 128:200401. doi:10.1103/PhysRevLett.128.200401
58. Yu J, Qin Y, Yan Z, Lu H, Jia X. Improvement of the intensity noise and frequency stabilization of Nd:YAP laser with an ultra-low expansion Fabry–Perot cavity. *Opt Express* (2019) 27:3247–54. doi:10.1364/OE.27.003247
59. Zhao B, Qin W, Li F, Lu H. All-solid-state CW single-frequency deep UV 266 nm laser. *J Quan Opt* (2020) 26:194–201. doi:10.3788/jqo20202602.0901
60. Yang X, Bai Z, Chen D, Chen W, Feng Y, Mildren RP. Widely-tunable single-frequency diamond Raman laser. *Opt Express* (2021) 29:29449–57. doi:10.1364/OE.435023
61. Nie D, Feng J, Li Y, Zhang K. Two-color quantum correlation between down-conversion beams at 1.5 and 3.3 μm from a singly resonant optical parametric oscillator. *Appl Sci* (2020) 10:2698. doi:10.3390/app10082698